crystals

MDPI

Communication

Structural Characterized Homotrinuclear Zn^{II} Bis(Salamo)-Based Coordination Compound: Hirshfeld Surfaces, Fluorescent and Antimicobial Properties

Yang Zhang, Ling-Zhi Liu, Ying-Qi Pan and Wen-Kui Dong *

School of Chemical and Biological Engineering, Lanzhou Jiaotong University, Lanzhou 730070, China; zhangy8124@163.com (Y.Z.); llz1009663202@126.com (L.-Z.L.); panyq0329@163.com (Y.-Q.P.)

* Correspondence: dongwk@126.com

Received: 22 May 2018; Accepted: 20 June 2018; Published: 22 June 2018

Abstract: A homotrinuclear Zn^{II} bis(salamo) coordination compound, $[LZn_3(OAc)_2(H_2O)]$ of a new bis(salamo)-like ligand, has been synthesized and structurally characterized using elemental analyses, IR, UV-Vis and fluorescent spectra, and Hirshfeld surface analysis. Hirshfeld surface analyses and X-ray crystallography revealed that complexation between Zn^{II} acetate dihydrate and the ligand H_4L afforded a 3:1 (Zn^{II}:L) type coordination compound. Moreover, the X-ray crystal structure analysis demonstrated that two μ_2-acetate anions bridge three Zn^{II} atoms in a μ_2-fashion forming a homo-trinuclear structure. There were two kinds of Zn^{II} atoms coordination geometries (strongly distorted square pyramidal (Zn1) and distorted trigonal bipyramidal (Zn2 and Zn3)) in the Zn^{II} coordination compound. In addition, a 3D supra-molecular structure was constructed by intermolecular C-H$\cdots\pi$ and $\pi\cdots\pi$ interactions in the Zn^{II} coordination compound. Most importantly, the fluorescent and antimicrobial properties of H_4L and its Zn^{II} coordination compound were investigated.

Keywords: Zn^{II} coordination compound; crystal structure; supra-molecular interaction; fluorescence property; antimicrobial activity

1. Introduction

In recent years, a great number of 3D metal coordination compounds with salen-like N_2O_2 ligands have been widely investigated [1–8]. More recently, salamo-like N_2O_2 chelating ligands and their analogues, using an *O*-alkyloxime (–CH=N–O–$(CH_2)_n$–O–N=CH–), have been explored [9–15]. Compared to salen-like coordination compounds, salamo-type coordination compounds are significantly more stable. The latter, salamo-like ligands, are more attractive candidates for metal-binding sites to be involved into metallohosts. Salamo-like ligands could coordinate to different transition metal ions in a tetradentate N_2O_2-type fashion to form stable metal coordination compounds, some of which are often as organic reaction catalysts [16], metal enzyme reaction center models [17,18], nonlinear optical and magnetic molecular materials [19–27], supramolecular architectures and host-guest chemistries [28–34], electrochemistries [35–37] and so on.

To utilize salamo units to control guest recognition, a better strategy distinguished from the macrocyclization has been proposed [38,39]. Thus, we designed and prepared a new C-shaped bis(salamo)-like chelating ligand that contained a O_4 site besides the two N_2O_2 sites, to control guest binding via using the coordination-triggered conformational changes. When the ligand is metalated, our O_4 oxygen atoms are located in an acyclic, C-shaped arrangement. Moreover, the guest binding could be more effective owing to the negatively charged phenolates of the metal coordination

compounds having higher coordination ability to other metals than their phenol form. Interestingly, some studies have been devoted to research mono-, multi-, homo- or heteromultinuclear metal coordination compounds bearing salamo-type ligands or their derivatives [40,41].

Herein, on the basis of our previous studies [42–46], we have studied cooperative formation of a trinuclear Zn^{II} bis(salamo)-like coordination compound, instead of the dinuclear bis(salamo)-like coordination compound reported before [47], via the metalation of bis(salamo)-like ligand H_4L. IR, UV-Vis titration and X-ray crystallography clearly exhibited that complexation between Zn^{II} acetate dihydrate and H_4L can form a 3:1 $[Zn_3L]^{2+}$ coordination compound. Meanwhile, the fluorescent and antibacterial properties of H_4L and its Zn^{II} coordination compound were also studied.

2. Experimental Section

2.1. Materials and Methods

2-Hydroxy-4-methoxybenzaldehyde (99%), 1,2-dibromopropane, 1,2-dimethoxybenzene, TMEDA, *n*-butyllithium, boron tribromide were bought from Alfa Aesar and used without further purification. Other solvents and reagents (DMF: *N*,*N*-dimethylformamide) were analytical grade reagents from Tianjin Chemical Reagent Factory.

C, H and N analyses were gained using a GmbH VariuoEL V3.00 automatic elemental analysis instrument (Elementar, Berlin, Germany). Elemental analysis for Zn^{II} was measured with an IRIS ER/S-WP–1 ICP atomic emission spectrometer (Elementar, Berlin, Germany). Melting points were obtained by the use of a microscopic melting point apparatus made by Beijing Taike Instrument Company Limited and were uncorrected. IR spectra (400–4000 cm^{-1}) were recorded on a Vertex 70 FT-IR spectrophotometer (Bruker, Billerica, MA, USA), with samples prepared as KBr pellets. UV-Vis absorption spectra were recorded on a Shimadzu UV-3900 spectrometer (Shimadzu, Tokyo, Japan). ^1H NMR spectra were determined by German Bruker AVANCE DRX-400/600 spectroscopy. Single crystal X-ray structure diffraction for the Zn^{II} coordination compound was carried out a Bruker Smart Apex CCD diffractometer. Fluorescent spectra were recorded on a F-7000 FL spectrophotometer.

2.2. Synthesis of the Ligand H_4L

A synthetic route to the new ligand H_4L is depicted in Scheme 1. Preparations of 2,3-dihydroxybenzene-1,4-dicarbaldehyde (1) and 2-[*O*-(1-ethyloxyamide)] oxime-5-methoxyphenol (**2**) were in accordance with the literature [48–52]. A ethanol solution (15 mL) of 2-[*O*-(1-ethyloxyamide)]oxime-5-methoxyphenol (452.46 mg, 2 mmol) was added dropwise to a ethanol solution (20 mL) of 2,3-dihydroxybenzene-1,4-dicarbaldehyde (166.13 mg, 1 mmol) under 55 °C, the mixture was heated to reflux and kept refluxing for 6 h, and then faint yellow solid of the bis(salamo)-like tetraoxime ligand (H_4L) was obtained. After the solution was allowed to stand overnight at room temperature, precipitates were collected on a suction filter to afford H_4L. Yield: 346.20 mg (65.5%). m.p. 148–149 °C. Anal. calcd. for $C_{28}H_{30}N_4O_{10}$ (%): C, 57.73; H, 5.19; N, 9.62. Found (%): C, 58.92; H, 5.44; N, 9.47. ^1H NMR (500 MHz, CDCl) δ 9.91 (s, 2H, OH), 9.66 (s, 2H, OH), 8.23 (s, 2H, CH=N), 8.18 (s, 2H, CH=N), 7.06 (s, 2H, ArH), 6.77 (s, 2H, ArH), 6.49 (s, 2H, ArH), 6.47 (dd, *J* = 8.5, 2.6 Hz, 2H, ArH), 4.50 (s, 4H, CH_2), 4.45 (s, 4H, CH_2), 3.81 (s, 6H, CH_3).

2.3. Synthesis of the Zn^{II} Coordination Compound

A solution of Zn^{II} acetate dihydrate (6.58 mg, 0.03 mmol) in methanol (1 mL) was added dropwise to a solution of H_4L (5.88 mg, 0.01 mmol) in dichloromethane (3 mL), the color of the mixture turned to yellow immediately, the proper solvent ratio (methanol:dichloromethane = 1:3) was of utmost importance. After 0.5 h of stirring, the resulting yellow solution was filtered, and then left undisturbed. When the solution was partially evaporated, several yellow block-like single crystals suitable for X-ray crystallography were gained. Yield: 54% (4.92 mg). Anal. calcd. for $C_{32}H_{34}Zn_3N_4O_{15}$ (%): C, 42.20; H, 3.76; N, 6.15; Zn, 21.54. Found (%): C, 42.41; H, 3.85; N, 6.02; Zn, 21.84.

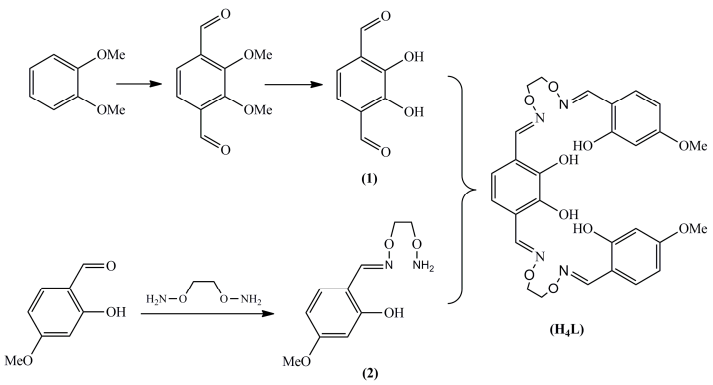

Scheme 1. Synthesis route of H_4L.

2.4. X-ray Crystallography

The single crystal of the Zn^{II} coordination compound, with approximate dimensions of 0.38 × 0.40 × 0.48 mm was mounted on goniometer head of Bruker Smart 1000 diffractometer equipped with Apex CCD area detector. The diffraction data were collected using a graphite mono-chromated Mo $K\alpha$ radiation (λ = 0.71073 Å) at 298(2) K. The structure was solved by using the program SHELXS-97 and Fourier difference techniques, and refined by full-matrix least-squares method on F^2 using SHELXL-2017. The structure contained large void, and the solvent and the positive or negative ions located in the void couldn't be identified because it was highly disordered and had so small residual peak. Therefore, SQUEEZE in PLATON program was performed to remove the highly disordered solvent and ions. (Solvent Accessible Volume = 1762.9, Electrons Found in S.A.V. = 104.2). The nonhydrogen atoms were refined anisotropically. Hydrogen atoms were added in geometrical positions. Details of the data collection and refinements of the Zn^{II} coordination compound are given in Table 1.

Table 1. Crystallographic data and collection parameters for the Zn^{II} coordination compound.

Empirical Formula	$C_{32}H_{34}Zn_3N_4O_{15}$
Formula weight	910.74
Temperature, K	298(2)
Wavelength, Å	0.71073
Crystal system	Monoclinic
Space group	C 2/c
Cell dimensions, (Å, deg)	a = 26.702(2) b = 21.6859(19), c = 14.8470(13), β = 101.253(2)
Volume, $Å^3$	8432.0(13)
Z	8
Density (calculated), mg/m^3	1.435
Absorption coefficient, mm^{-1}	1.759
F(000)	3712.0
Index ranges	$-28 \leq h \leq 31$, $-22 \leq k \leq 25$, $-17 \leq l \leq 16$
Reflections collected	20,924/7426 [R(int) = 0.0496]
Independent reflections	5335
Data/restraints/parameters	7426/36/514
Goodness of fit indicator	0.944
R [$I > 2\sigma(I)$]	R_1 = 0.0366, wR_2 = 0.0903
Largest diff. peak and hole, e·$Å^{-3}$	0.357 and −0.382

$R_1 = \Sigma||F_o| - |F_c||/\Sigma|F_o|$; $wR_2 = [\Sigma w(F_o^2 - F_c^2)^2/\Sigma w(F_o^2)^2]^{1/2}$, $w = [\sigma^2(F_o^2) + (0.0784P)^2 + 1.3233P]^{-1}$, where $P = (F_o^2 + 2F_c^2)/3$; GOF = $[\Sigma w(F_o^2 - F_c^2)^2/n_{obs}\text{-}n_{param})]^{1/2}$.

Supplementary crystallographic data have been deposited at Cambridge Crystallographic Data Centre (CCDC: 890890). Copies of the data could be gained free of charge on application to CCDC, 12 Union Road, Cambridge CB21EZ, UK (Telephone: +44-01223-762910; Fax: +44-1223-336033; E-mail: deposit@ccdc.cam.ac.uk). The data could be also gained free of charge at www.ccdc.cam.ac.uk/conts/retrieving.html.

3. Results and Discussion

3.1. IR Spectra

As depicted in Figure 1, the IR spectra of H_4L and its Zn^{II} coordination compound exhibited different bands in the 4000–500 cm^{-1} region. A typical C=N stretching band of H_4L appeared at 1626 cm^{-1}, however that of the Zn^{II} coordination compound was observed at 1597 cm^{-1}, indicating that the oxime nitrogen atoms are coordinated to the Zn^{II} atoms [53–57].

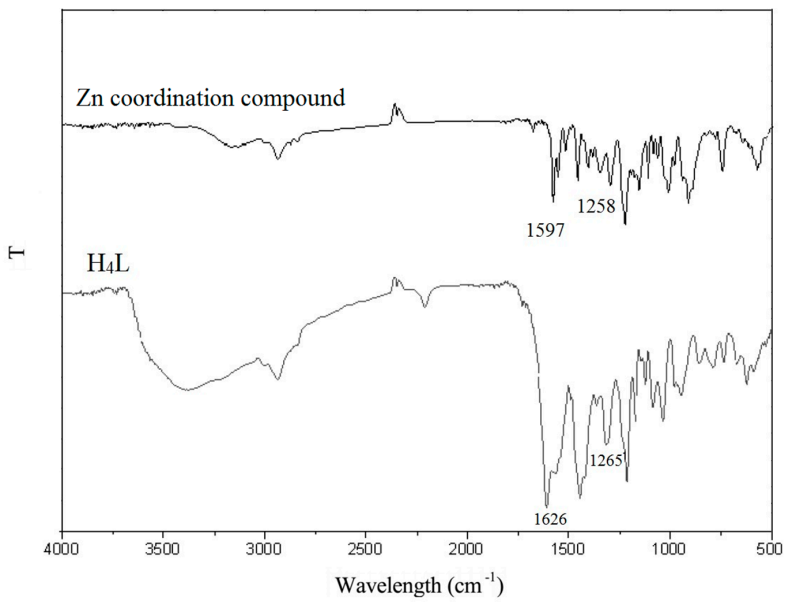

Figure 1. IR spectra of the ligand H_4L and its Zn^{II} coordination compound.

Meanwhile, the free ligand H_4L displayed a typical Ar–O stretching frequency at 1265 cm^{-1}, while the Ar–O stretching frequency of the Zn^{II} coordination compound was observed at 1258 cm^{-1}. This frequency was shifted to high frequency, which can be an evidence of formation of the Zn^{II}–O bonds between the Zn^{II} atoms and the phenolic oxygen atoms [58–60].

3.2. UV-Vis Absorption Spectra

UV-Vis absorption spectra of the ligand H_4L and its Zn^{II} coordination compound were measured in 5×10^{-5} mol/L DMF solution (Figure 2).

In the UV-Vis titration experiment of the Zn^{II} coordination compound, the spectroscopic titration clearly showed the reaction stoichiometry ratio to be 3:1. Absorption spectra of the Zn^{II} coordination compound were clearly different from that of H_4L upon complexation. The absorption maxima at ca. 278 and 313 nm were shifted bathochromically upon coordination to the Zn^{II} atoms, and a new absorption maxima at ca. 444 nm was absent in the spectrum of the Zn^{II} coordination compound, which should be assigned to LMCT [61–65].

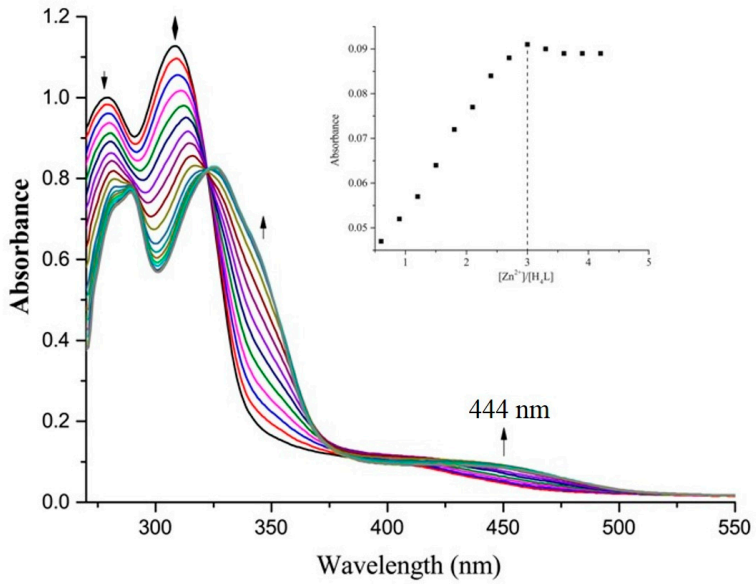

Figure 2. Absorption spectra of H_4L in DMF with the increase of Zn^{II}. Inset: the absorbance at 444 nm varied as a function of $[Zn^{2+}]/[H_4L]$. $[H_4L] = 5 \times 10^{-5}$ mol/L.

3.3. Crystal Structure Description

From a 3:1 mixture of Zn^{II} acetate dihydrate and the ligand H_4L, a yellow crystalline coordination compound was obtained. X-ray crystallography obviously displayed that the Zn^{II} coordination compound included one completely deprotonated ligand $(L)^{4-}$ unit, three Zn^{II} atoms, two μ_2-acetate ligands, and one coordinated water molecule (Figure 3).

Two of the three Zn^{II} (Zn2 and Zn3) atoms sat in the salamo N_2O_2 moieties, while Zn1 was located in the central O_4 site. Two oxygen (O1 and O2) atoms bridged Zn1-Zn2 and Zn1-Zn3, respectively. In addition, two μ_2-acetato ligands linked Zn1 to Zn2 and Zn1 to Zn3 stabilizing the homotrinuclear structure. The central Zn^{II} (Zn1) atom was found to have an aqua molecule. Thus, two of the three Zn^{II} (Zn2 and Zn3) atoms possess pentacoordinate distorted trigonal bipyramidal geometries ($\tau = 0.8038$) in which the axial positions were held by N2-O1 and N4-O2, respectively. Besides, Zn1 atom possesses a strongly distorted square pyramidal ($\tau = 0.3128$) coordination environment where the axial position was held by the O15 atom of the aqua molecule [17,23]. Selected bond distances and angles are listed in Table 2. It can be seen from the data that the different positions of the substituents can lead to slightly different changes in the structure [11].

Table 2. Selected bond lengths (Å) and angles (°) for the Zn^{II} coordination compound.

Bond	Lengths	Bond	Lengths	Bond	Lengths
Zn1-O11	1.975(3)	Zn1-O13	1.998(3)	Zn1-O15	2.021(3)
Zn1-O2	2.042(2)	Zn1-O1	2.079(2)	Zn2-O5	1.962(2)
Zn2-O12	1.985(3)	Zn2-O1	2.052(2)	Zn2-N1	2.091(3)
Zn2-N2	2.135(3)	Zn3-O9	1.959(3)	Zn3-O14	1.971(3)
Zn3-O2	2.057(2)	Zn3-N4	2.104(3)	Zn3-N3	2.150(3)
Bond	**Angles**	**Bond**	**Angles**	**Bond**	**Angles**
O11-Zn1-O13	89.62(13)	O11-Zn1-O15	114.09(13)	O13-Zn1-O15	99.82(11)
O11-Zn1-O2	145.43(15)	O13-Zn1-O2	93.15(10)	O15-Zn1-O2	99.38(9)
O11-Zn1-O1	88.93(11)	O13-Zn1-O1	164.20(13)	O15-Zn1-O1	95.13(10)
O2-Zn1-O1	79.31(9)	O5-Zn2-O12	114.15(11)	O5-Zn2-O1	92.43(9)
O12-Zn2-O1	90.61(10)	O5-Zn2-N1	126.79(11)	O12-Zn2-N1	118.97(11)
O1-Zn2-N1	84.29(10)	O5-Zn2-N2	87.16(10)	O12-Zn2-N2	94.10(11)
O1-Zn2-N2	175.02(10)	N1-Zn2-N2	91.98(11)	O9-Zn3-O14	112.13(11)
O9-Zn3-O2	93.72(10)	O14-Zn3-O2	95.00(10)	O9-Zn3-N4	88.47(11)
O14-Zn3-N4	96.81(11)	O9-Zn3-N3	121.50(11)	O2-Zn3-N3	81.51(10)
O2-Zn3-N4	166.17(11)	O14-Zn3-N3	126.37(11)	N4-Zn3-N3	85.70(12)

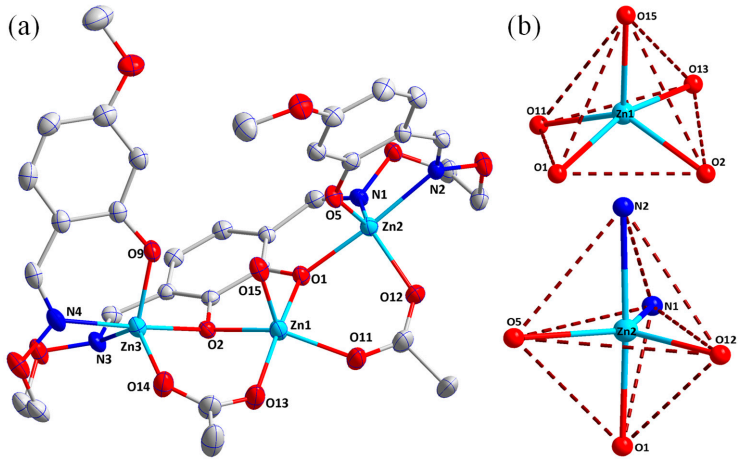

Figure 3. (**a**) Representation of the Zn^{II} coordination compound structure; (**b**) The coordination polyhedra of Zn1 and Zn2 centers.

3.4. Supra-Molecular Interaction

As illustrated in Table 3 and Figure 4, there were four pairs of intra-molecular O15-H15B···O9, O15-H15B···O5, C10-H10A···O12 and C20-H20B···O14 hydrogen bond interactions and a pair of C-H···π inter-molecular hydrogen bonds in the Zn^{II} coordination compound. The Zn^{II} coordination compound molecules were inter-linked effectively via C-H···π hydrogen bonds (C19-H19B···Cg1) into a 1D supermolecular structure. Furthermore, one molecule could link four adjacent molecules into an infinite 3D net-like supramolecular structure by two pairs of intermolecular Cg1···Cg1 and Cg3···Cg3 interactions [66–72]. The weak hydrogen bonds existing in the Zn^{II} coordination compound have been described in graph sets (Figure 5) [73]. Additionally, the hydrogen bonding scheme of the Zn^{II} coordination compound is defective due to suppression of the electron density originating from solvent molecules (used SQUEEZE) and subsequent exclusion of these solvent molecules from the refinement model.

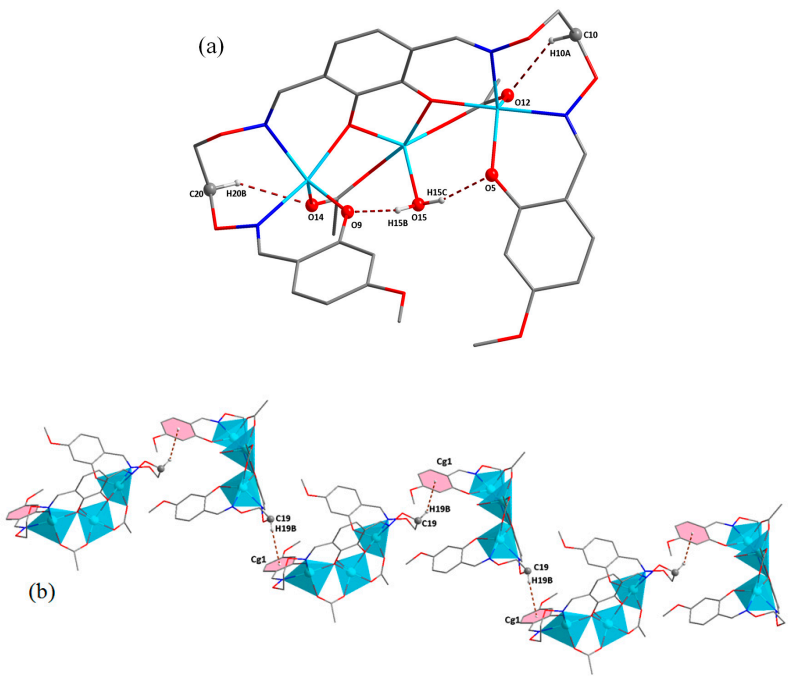

Figure 4. *Cont.*

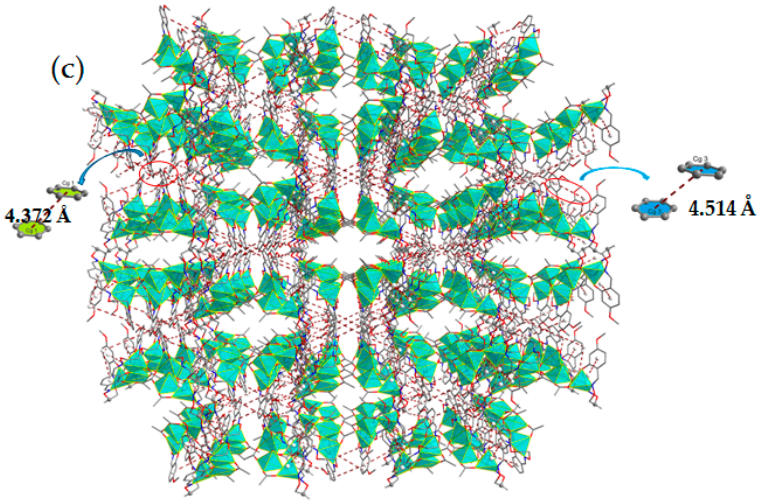

Figure 4. (**a**) Intra-molecular hydrogen bondings of the Zn^{II} coordination compound unit (hydrogen atoms, except those forming hydrogen bonds, are omitted for clarity); (**b**) One-dimensional supra-molecular structure of the Zn^{II} coordination compound, mediated by inter-molecular C-H···π (pink) interactions; (**c**) 3-D supramolecular structure of the Zn^{II} coordination compound, mediated by intermolecular C-H···π and π···π interactions.

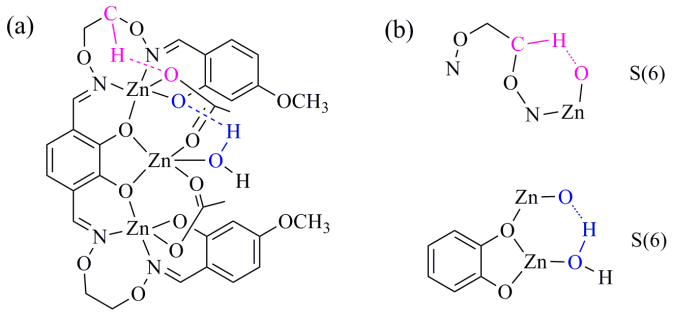

Figure 5. (**a**) Graph set assignments for the Zn^{II} coordination compound; (**b**) Partial enlarged drawing of hydrogen bonds.

Table 3. Hydrogen bonding and π···π stacking interactions [Å, °] for the Zn^{II} coordination compound.

D–H···A	d(D–H)	d(H–A)	d(D–A)	∠D–X–A	Symmetry Code
O15–H15B···O9	0.85	1.84	2.675(4)	168	
O15–H15C···O5	0.85	1.80	2.625(4)	162	
C10–H10A···O12	0.97	2.49	3.367(5)	150	
C20–H20B···O14	0.97	2.42	3.296(6)	150	
C19-H19B···Cg1	0.97	2.84	3.601(5)	136	1/2 − X, 1/2 + Y, 1/2 − Z
Cg1···Cg1			4.372		1/2 − X, 1/2 − Y, 1 − Z
Cg3···Cg3			4.541		1/2 − X, 1/2 − Y, −Z

Note: Cg1 is the centroids for benzene ring C12–C17, Cg3 is the centroids for benzene ring C22–C27.

3.5. Hirshfeld Surfaces

The Hirshfeld surfaces of the Zn^{II} coordination compound are depicted in Figure 6, exhibiting surfaces that have been mapped over d_{norm} and d_i [74,75]. The interactions between hydroxyl oxygen in the Zn^{II} coordination compound can be seen as bright red areas in the Hirshfeld surface in Figure 7.

The light red spots are owing to C–H···O interactions, and other visible spots correspond to C···H and H···H contacts on the surface. Figure 7 shows the 2D plots generated [76–78] which correspond to the C···H, O···H and H···H interactions from the Hirshfeld surface of the Zn^{II} coordination compound. To provide context, the overview of the full fingerprint is depicted in grey and the blue area showing the separate contact. The proportions of O···H/H···O, C···H/H···C and H···H interactions are composed of 22.3, 12.1 and 49.7% of the all Hirshfed surfaces for each Zn^{II} coordination compound molecule, respectively. It is because of the existence of these hydrogen bondings that the Zn^{II} coordination compound can be stable.

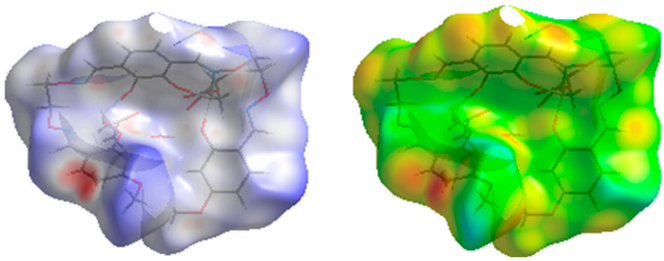

(a) (b)

Figure 6. Hirshfeld surfaces mapped with (**a**) d_{norm} and (**b**) d_i of the Zn^{II} coordination compound. The surfaces are depicted as transparent to allow visualization of the molecule structure.

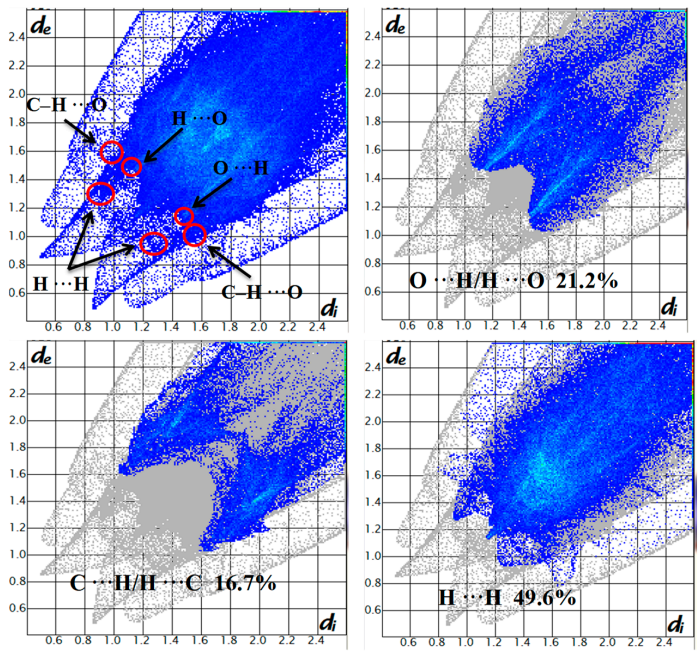

Figure 7. Fingerprint plot of the Zn^{II} coordination compound: full and resolved into full and resolved into O···H, C···H and H···H contacts exhibiting the percentages of contacts contributed to the total Hirshfeld surface area of the Zn^{II} coordination compound molecule.

3.6. Fluorescent Spectra

The fluorescence titration experiment of the Zn^{II} coordination compound with H_4L was studied. Figure 8 shows gradual changes in the fluorescence spectra of H_4L upon addition of Zn^{II} ions. The ligand exhibited an intense emission at ca. 525 nm upon excitation at 380 nm based on global maximum determined from three-dimensional fluorescence spectra, which could be attributed to

intra-lignd π–π* transition [79–81]. Figure 8 obviously indicates that fluorescence emission of the ligand H_4L was very weak, probably owing to isomerization of C=N double bond, intramolecular hydrogen bond between azomethine and hydroxyl moieties of the aromatic group. Upon incremental addition of Zn^{II} ions to the solution of H_4L, fluorescence emission intensity at 523 nm gradually increased, and this peak remained relatively constant after the addition of 3 equiv.

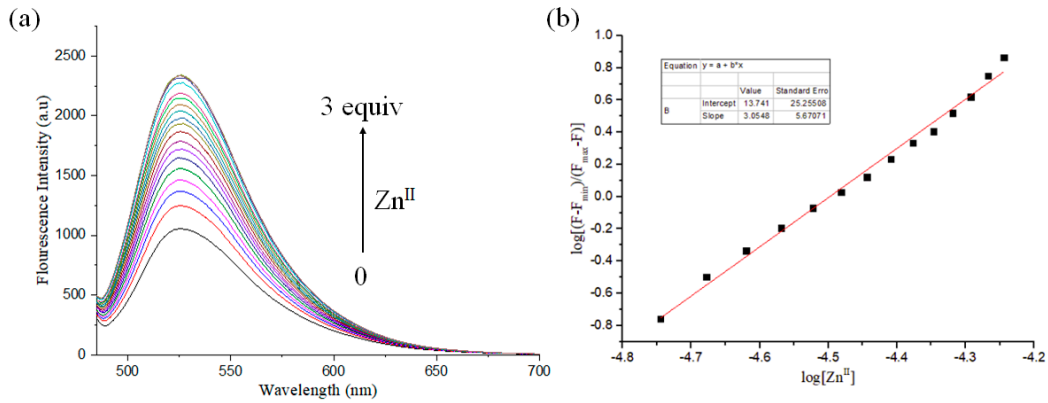

Figure 8. (**a**) Fluorescence spectrum changes of the H_4L solution (c = 5 × 10^{-5} mol/L) upon addition of different amounts of Zn^{II} ions (0–3.0 equiv) in dilute dichloromethane:methanol (*v*:*v* = 1:1) solutions at room temperature; (**b**) The linear relationship between fluorescence intensity and the concentrations of Zn^{II} ions. (λ_{ex} = 380 nm, λ_{em} = 523 nm).

The Zn^{II} coordination compound showed a strong and broad luminescence with maximum emission at ca. 523 nm upon excitation at 380 nm, which is moved bathochromically to that of H_4L. Compared with the emission spectrum of H_4L, enhanced fluorescent intensity of the Zn^{II} coordination compound was observed, displaying that intra-ligand transition has been affected owing to the introduction of the Zn^{II} atoms [82,83]. No emissions coming from ligand-to-metal/metal-to-ligand charge-transfer or metal-centered excited states are expected for the Zn^{II} coordination compound, since Zn^{II} is a d^{10} ion. Therefore, the emission of the Zn^{II} coordination compound observed is tentatively assigned to the intra-ligand π–π* fluorescence. From the emission intensity by following the modified Benesi–Hidebrand equation, the association constant of compound was calculated as 1.59 × 10^4 M^{-1} [31–34].

3.7. Antimicobial Activities

The antimicrobial properties of H_4L and its Zn^{II} coordination compound were detected against *Escherichia coli* as *Staphylococcus aureus* and Gram-negative bacteria as Gram-positive bacteria via a punch method. The bacterial suspension was mixed in sterile LB (lysogeny broth agar) plates (2% agar), then made four holes with a hole punch, last added DMF, Zn^{2+}, H_4L, and the Zn^{II} coordination compound into every holes. After 7 h of incubation at 37 °C, the growth-inhibitory effect was monitored and diameters of the inhibition zones were measured. The discs measuring 5 mm in diameter were dissolved in DMF. The diameters of inhibition zones of H_4L and its Zn^{II} coordination compound are given in Figure 9, the Zn^{II} coordination compound proved more enhanced antimicrobial activities than the bis(salamo)-like tetraoxime H_4L under the same concentrations.

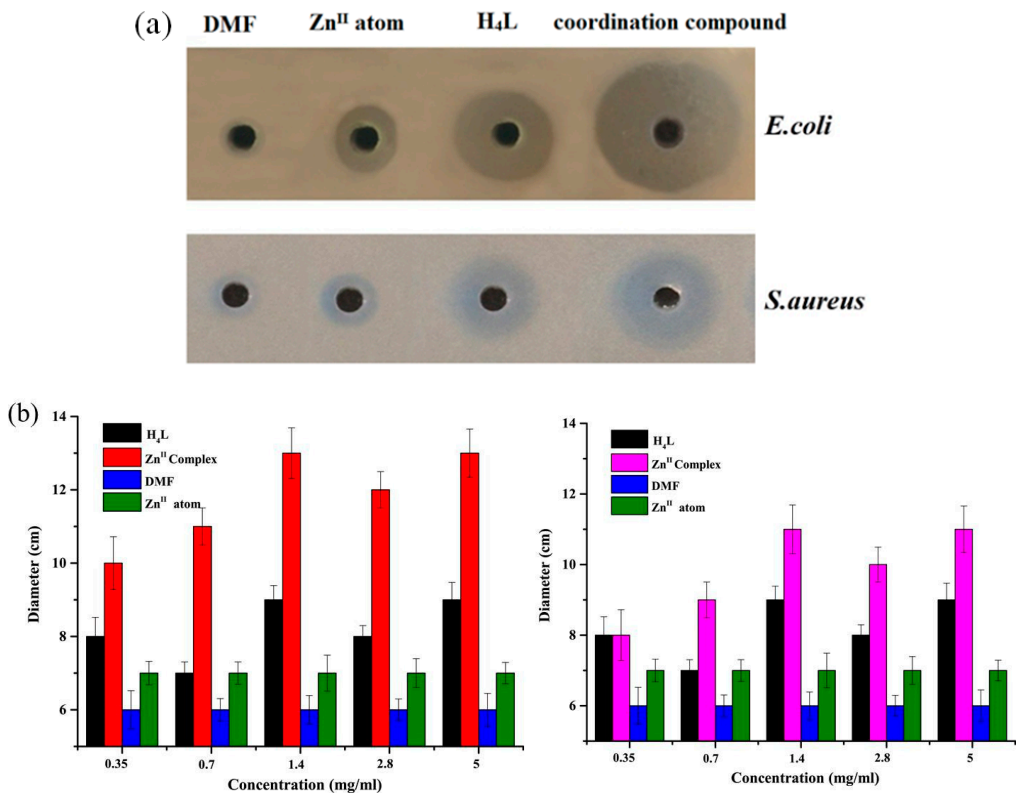

Figure 9. (**a**) The diameters of inhibition zones of *E. coli* and *S. aureus* at different concentrations; (**b**) the diameter of inhibition zones of *E. coli* and *S. aureus* in different concentrations.

As shown in Figure 9, the inhibitory effect of the Zn^{II} coordination compound at different concentrations was studied, the results showed that the antibacterial effect of the Zn^{II} coordination compound increased with increasing concentrations. The increase in the antibacterial activity of the Zn^{II} coordination compound with increase in concentration can be explained according to the chelation theory. Chelation reduces the polarity of the metal atom mainly owing to partial sharing of positive charge of Zn^{II} atom with donor groups and possible delocalization of π-electron within the whole chelate ring. Further, it enhances the lipophilic character of the central atom. These results are similar to earlier reports of biological activities of similar salamo-like Co^{II} coordination compounds [84].

4. Conclusions

A newly designed symmetric bis(salamo)-like chelating tetraoxime ligand H_4L, possessing a C-shaped O_4 site besides the two N_2O_2 sites, has been synthesized, and its Zn^{II} coordination compound $[LZn_3(OAc)_2(H_2O)]$ has been determined by X-ray crystallography. The UV-Vis titration experiment clearly showed the reaction stoichiometry ratio to be 3:1. In the Zn^{II} coordination compound, Zn1 is pentacoordinate with a strongly distorted square pyramidal geometry, while Zn2 and Zn3 possess pentacoordinates with distorted trigonal bipyramidal geometries. Furthermore, the Hirshfeld surface analysis indicated that the Zn^{II} coordination compound could be stable due to intramolecular hydrogen bonds and some weaker interactions. Fluorescence behaviors of H_4L and its Zn^{II} coordination compound were investigated, compared with the ligand H_4L, the emission intensity of the Zn^{II} coordination compound increased obviously, which indicated that the Zn^{II} ions possess a quality of fluorescent enhancement. Antimicrobial experiments showed that the Zn^{II} coordination compound demonstrated more enhanced antimicrobial activities than H_4L under the same conditions.

Author Contributions: W.-K.D. conceived and designed the experiments; Y.Z. performed the experiments; Y.-Q.P. analyzed the data; L.-Z.L. contributed reagents/materials/analysis tools; Y.Z. wrote the paper.

Funding: This work was supported by the Program for Excellent Team of Scientific Research in Lanzhou Jiaotong University, 201706; National Natural Science Foundation of China, 21761018.

Acknowledgments: This work was supported by the National Natural Science Foundation of China (21761018) and the Program for Excellent Team of Scientific Research in Lanzhou Jiaotong University (201706), both of which are gratefully acknowledged.

Conflicts of Interest: The authors declare no conflict of interests.

References

1. Shu, Y.B.; Liu, W.S. Luminescent chiral Eu(III) complexes with enantiopurebis(1H-pyridin-2-one)salen ligands. *Polyhedron* **2015**, *102*, 293–296. [CrossRef]
2. Liu, P.P.; Sheng, L.; Song, X.Q.; Xu, W.Y.; Liu, Y.A. Synthesis, structure and magnetic properties of a new one dimensional manganese coordination polymer constructed by a new asymmetrical ligand. *Inorg. Chim. Acta* **2015**, *434*, 252–257. [CrossRef]
3. Ma, X.; Jiao, J.M.; Yang, J.; Huang, X.B.; Cheng, Y.X.; Zhu, C.J. Large stokes shift chiral polymers containing (*R*,*R*)-salen-based binuclear boron complex: Synthesis, characterization, and fluorescence properties. *Polyhedron* **2012**, *53*, 3894–3899. [CrossRef]
4. Wu, H.L.; Wang, C.P.; Wang, F.; Peng, H.P.; Zhang, H.; Bai, Y.C. A new manganese (III) complex from bis(5-methylsalicylaldehyde)-3-oxapentane-1,5-diamine: Synthesis, characterization, antioxidant activity and luminescence. *J. Chin. Chem. Soc.* **2015**, *62*, 1028–1034. [CrossRef]
5. Wang, F.; Xu, Y.L.; Aderinto, S.O.; Peng, H.P.; Zhang, H.; Wu, H.L. A new highly effective fluorescent probe for Al^{3+} ions and its application in practical samples. *J. Photochem. Photobiol. A* **2017**, *332*, 273–282. [CrossRef]
6. Lee, S.H.; Shin, N.; Kwak, S.W.; Hyun, K.; Woo, W.H.; Lee, J.H.; Hwang, H.; Kim, M.; Lee, J.; Kim, Y.; et al. Intriguing indium-salen complexes as multicolor luminophores. *Inorg. Chem.* **2017**, *56*, 2621–2626. [CrossRef] [PubMed]
7. Zhou, J.J.; Song, X.Q.; Liu, Y.A.; Wang, X.L. Substituent-tuned structure and luminescence sensitizing towards Al^{3+} based on phenoxy bridged dinuclear Eu^{III} complexes. *RSC Adv.* **2017**, *7*, 25549–25559. [CrossRef]
8. Chakraborty, A.; Bag, P.; Goura, J.; Bar, A.K.; Sutter, J.-P.; Chandrasekhar, V. Chair-shaped $Mn^{II}{}_2Ln^{III}{}_4$ (Ln = Gd, Tb, Dy, Ho) heterometallic complexes assembled from a tricompartmental aminobenzohydrazide ligand. *Cryst. Growth Des.* **2015**, *15*, 848–857. [CrossRef]
9. Akine, S.; Sairenji, S.; Taniguchi, T.; Nabeshima, T. Stepwise helicity inversions by multisequential metal exchange. *J. Am. Chem. Soc.* **2013**, *135*, 12948–12951. [CrossRef] [PubMed]
10. Akine, S.; Taniguchi, T.; Saiki, T.; Nabeshima, T. Ca^{2+}- and Ba^{2+}-selective receptors based on site-selective transmetalation of multinuclear polyoxime-zinc(II) complexes. *J. Am. Chem. Soc.* **2005**, *127*, 540–541. [CrossRef] [PubMed]
11. Akine, S.; Taniguchi, T.; Nabeshima, T. Helical metallohost-guest complexes via site-selective transmetalation of homotrinuclear complexes. *J. Am. Chem. Soc.* **2006**, *128*, 15765–15774. [CrossRef] [PubMed]
12. Dong, W.K.; Ma, J.C.; Dong, Y.J.; Zhu, L.C.; Zhang, Y. Di- and tetranuclear heterometallic 3d–4f cobalt(II)–lanthanide(III) complexes derived from a hexadentate bisoxime: Syntheses, structures and magnetic properties. *Polyhedron* **2016**, *115*, 228–235. [CrossRef]
13. Dong, W.K.; Tong, J.F.; Sun, Y.X.; Wu, J.C.; Yao, J.; Gong, S.S. Studies on mono- and dinuclear bisoxime copper complexes with different coordination geometries. *Transit. Met. Chem.* **2010**, *35*, 419–426. [CrossRef]
14. Dong, W.K.; Wang, Z.K.; Li, G.; Zhao, M.M.; Dong, X.Y.; Liu, S.H. Syntheses, crystal structures, and properties of a Salamo-type tetradentate chelating ligand and its pentacoordinated copper(II) complex. *Z. Anorg. Allg. Chem.* **2013**, *639*, 2263–2268. [CrossRef]
15. Akine, S.; Taniguchi, T.; Nabeshima, T. Synthesis and characterization of novel ligands 1,2-bis(salicylideneaminooxy)ethanes. *Chem. Lett.* **2001**, *30*, 682–683. [CrossRef]
16. Chai, L.Q.; Wang, G.; Sun, Y.X.; Dong, W.K.; Zhao, L.; Gao, X.H. Synthesis, crystal structure, and fluorescence of an unexpected dialkoxo-bridged dinuclear copper(II) complex with bis(salen)-type tetraoxime. *J. Coord. Chem.* **2012**, *65*, 1621–1631. [CrossRef]

17. Chen, L.; Dong, W.K.; Zhang, H.; Zhang, Y.; Sun, Y.X. Structural variation and luminescence properties of tri- and dinuclear Cu^{II} and Zn^{II} complexes constructed from a naphthalenediol-based bis(Salamo)-type ligand. *Cryst. Growth Des.* **2017**, *17*, 3636–3648. [CrossRef]
18. Li, L.H.; Dong, W.K.; Zhang, Y.; Akogun, S.F.; Xu, L. Syntheses, structures and catecholase activities of homo- and hetero-trinuclear cobalt(II) complexes constructed from an acyclic naphthalenediol-based bis(Salamo)-type ligand. *Appl. Organomet. Chem.* **2017**, e3818. [CrossRef]
19. Dong, W.K.; Zhang, J.; Zhang, Y.; Li, N. Novel multinuclear transition metal(II) complexes based on an asymmetric Salamo-type ligand: Syntheses, structure characterizations and fluorescent properties. *Inorg. Chim. Acta* **2016**, *444*, 95–102. [CrossRef]
20. Dong, W.K.; Zhang, L.S.; Sun, Y.X.; Zhao, M.M.; Li, G.; Dong, X.Y. Synthesis, crystal structure and spectroscopic properties of a supramolecular zinc(II) complex with N_2O_2 coordination sphere. *Spectrochim. Acta Part A* **2014**, *121*, 324–329. [CrossRef] [PubMed]
21. Gao, L.; Wang, F.; Zhao, Q.; Zhang, Y.; Dong, W.K. Mononuclear Zn(II) and trinuclear Ni(II) complexes derived from a coumarin-containing N_2O_2 ligand: Syntheses, crystal structures and fluorescence properties. *Polyhedron* **2018**, *139*, 7–16. [CrossRef]
22. Hao, J.; Liu, L.Z.; Dong, W.K.; Zhang, J.; Zhang, Y. Three multinuclear Co(II), Zn(II) and Cd(II) complexes based on a single-armed salamo-type bisoxime: Syntheses, structural characterizations and fluorescent properties. *J. Coord. Chem.* **2017**, *11*, 1936–1952. [CrossRef]
23. Zheng, S.S.; Dong, W.K.; Zhang, Y.; Chen, L.; Ding, Y.J. Four Salamo-type 3d–4f hetero-bimetallic [$Zn^{II}Ln^{III}$] complexes: Syntheses, crystal structures, and luminescent and magnetic properties. *New J. Chem.* **2017**, *41*, 4966–4973. [CrossRef]
24. Dong, W.K.; Zheng, S.S.; Zhang, J.T.; Zhang, Y.; Sun, Y.X. Luminescent properties of heterotrinuclear 3d–4f complexes constructed from a naphthalenediol-based acyclic bis(salamo)-type ligand. *Spectrochim. Acta Part A* **2017**, *184*, 141–150. [CrossRef] [PubMed]
25. Dong, W.K.; Ma, J.C.; Dong, Y.J.; Zhao, L.; Zhu, L.C.; Sun, Y.X.; Zhang, Y. Two hetero-trinuclear Zn(II)-M(II) (M = Sr, Ba) complexes based on metallohost of mononuclear Zn(II) complex: Syntheses, structures and fluorescence properties. *J. Coord. Chem.* **2016**, *69*, 3231–3241. [CrossRef]
26. Zhang, H.; Dong, W.K.; Zhang, Y.; Akogun, S.F. Naphthalenediol-based bis(Salamo)-type homo- and hetero-trinuclear cobalt(II) complexes: Syntheses, structures and magnetic properties. *Polyhedron* **2017**, *133*, 279–293. [CrossRef]
27. Dong, W.K.; Ma, J.C.; Zhu, L.C.; Zhang, Y. Nine self-assembled nickel(II)-lanthanide(III) heterometallic complexes constructed from a salamo-type bisoxime and bearing a N- or O-donor auxiliary ligand: Syntheses, structures and magnetic properties. *New J. Chem.* **2016**, *40*, 6998–7010. [CrossRef]
28. Dong, W.K.; Ma, J.C.; Zhu, L.C.; Zhang, Y. Self-assembled zinc(II)-lanthanide(III) heteromultinuclear complexes constructed from 3-MeOsalamo ligand: Syntheses, structures and luminescent properties. *Cryst. Growth Des.* **2016**, *16*, 6903–6914. [CrossRef]
29. Wang, F.; Gao, L.; Zhao, Q.; Zhang, Y.; Dong, W.K.; Ding, Y.J. A highly selective fluorescent chemosensor for CN^- based on a novel bis(salamo)-type tetraoxime ligand. *Spectrochim. Acta Part A* **2018**, *190*, 111–115. [CrossRef] [PubMed]
30. Dong, X.Y.; Li, X.Y.; Liu, L.Z.; Zhang, H.; Ding, Y.J.; Dong, W.K. Tri- and hexanuclear heterometallic Ni(II)-M(II) (M = Ca, Sr and Ba) bis(salamo)-type complexes: Synthesis, structure and fluorescence properties. *RSC Adv.* **2017**, *7*, 48394–48403. [CrossRef]
31. Dong, Y.J.; Li, X.L.; Zhang, Y.; Dong, W.K. A highly selective visual and fluorescent sensor for Pb^{2+} and Zn^{2+} and crystal structure of Cu^{2+} complex based-on a novel single-armed salamo type bisoxime. *Supramol. Chem.* **2017**, *29*, 518–527. [CrossRef]
32. Wang, B.J.; Dong, W.K.; Zhang, Y.; Akogun, S.F. A novel relay-sensor for highly sensitive and selective detection of Zn^{2+}/Pic^- and fluorescence on/off switch response of H^+/OH^-. *Sens. Actuators B Chem.* **2017**, *247*, 254–264. [CrossRef]
33. Dong, W.K.; Akogun, S.F.; Zhang, Y.; Sun, Y.X.; Dong, X.Y. A reversible "turn-on" fluorescent sensor for selective detection of Zn^{2+}. *Sens. Actuators B Chem.* **2017**, *238*, 723–734. [CrossRef]
34. Dong, W.K.; Li, X.L.; Wang, L.; Zhang, Y.; Ding, Y.J. A new application of salamo-type bisoximes: As a relay-sensor for Zn^{2+}/Cu^{2+} and its novel complexes for successive sensing of H^+/OH^-. *Sens. Actuators B Chem.* **2016**, *229*, 370–378. [CrossRef]

35. Chai, L.Q.; Huang, J.J.; Zhang, H.S.; Zhang, Y.L.; Zhang, J.Y.; Li, Y.X. An unexpected cobalt(III) complex containing a Schiff base ligand: Synthesis, crystal structure, spectroscopic behavior, electrochemical property and SOD-like activity. *Spectrochim. Acta Part A* **2014**, *131*, 526–531. [CrossRef] [PubMed]
36. Chai, L.Q.; Tang, L.J.; Chen, L.C.; Huang, J.J. Structural, spectral, electrochemical and DFT studies of two mononuclear manganese(II) and zinc(II) complexes. *Polyhedron* **2017**, *122*, 228–240. [CrossRef]
37. Chai, L.Q.; Zhang, K.Y.; Tang, L.J.; Zhang, J.Y.; Zhang, H.S. Two mono- and dinuclear Ni(II) complexes constructed from quinazoline-type ligands: Synthesis, x-ray structures, spectroscopic, electrochemical, thermal, and antimicrobial studies. *Polyhedron* **2017**, *130*, 100–107. [CrossRef]
38. Chai, L.Q.; Li, Y.X.; Chen, L.C.; Zhang, J.Y.; Huang, J.J. Synthesis, X-ray structure, spectroscopic, electrochemical properties and DFT calculation of a bridged dinuclear copper(II) complex. *Inorg. Chim. Acta* **2016**, *444*, 193–201. [CrossRef]
39. Akine, S.; Hashimoto, D.; Saiki, T.; Nabeshima, T. Synthesis and structure of polyhydroxyl rigid triangular nano-macrocyclic imine having multiple hydrogen-bonding sites. *Tetrahedron Lett.* **2004**, *45*, 4225–4227. [CrossRef]
40. Akine, S.; Matsumoto, T.; Taniguchi, T.; Nabeshima, T. Synthesis, structures, and magnetic properties of tri- and dinuclear copper(II)-gadolinium(III) complexes of linear oligooxime ligands. *Inorg. Chem.* **2005**, *44*, 3270–3274. [CrossRef] [PubMed]
41. Akine, S.; Taniguchi, T.; Matsumoto, T.; Nabeshima, T. Guest-dependent inversion rate of a tetranuclear single metallohelicate. *Chem. Commun.* **2006**, 4961–4963. [CrossRef] [PubMed]
42. Akine, S.; Nabeshima, T. Cyclic and acyclic oligo(N_2O_2) ligands for cooperative multi-metal complexation. *Dalton Trans.* **2009**, 10395–10408. [CrossRef] [PubMed]
43. Li, X.Y.; Chen, L.; Gao, L.; Zhang, Y.; Akogun, S.F.; Dong, W.K. Syntheses, crystal structures and catalytic activities of two solvent-induced homotrinuclear Co(II) complexes with a naphthalenediol-based bis(salamo)-type tetraoxime ligand. *RSC Adv.* **2017**, *7*, 35905–35916. [CrossRef]
44. Hao, J.; Li, L.L.; Zhang, J.T.; Akogun, S.F.; Wang, L.; Dong, W.K. Four homo- and hetero-bismetallic 3d/3d-2s complexes constructed from a naphthalenediol-based acyclic bis(salamo)-type tetraoxime ligand. *Polyhedron* **2017**, *134*, 1–10. [CrossRef]
45. Dong, Y.J.; Dong, X.Y.; Dong, W.K.; Zhang, Y.; Zhang, L.S. Three asymmetric salamo-type copper(II) and cobalt(II) complexes: Syntheses, structures, fluorescent properties. *Polyhedron* **2017**, *123*, 305–315. [CrossRef]
46. Tao, C.H.; Ma, J.C.; Zhu, L.C.; Zhang, Y.; Dong, W.K. Heterobimetallic 3d–4f Zn(II)–Ln(III) (Ln = Sm, Eu, Tb and Dy) complexes with a N_2O_4 bisoxime chelate ligand and a simple auxiliary ligand Py: Syntheses, structures and luminescence properties. *Polyhedron* **2017**, *128*, 38–45. [CrossRef]
47. Peng, Y.D.; Wang, F.; Gao, L.; Dong, W.K. Structurally characterized dinuclear zinc(II) bis(salamo)-type tetraoxime complex possessing square pyramidal and trigonal bipyramidal geometries. *J. Chin. Chem. Soc.* **2018**, 1–7. [CrossRef]
48. Wang, L.; Ma, J.C.; Dong, W.K.; Zhu, L.C.; Zhang, Y. A novel self-assembled nickel(II)-cerium(III) heterotetranuclear dimer constructed from N_2O_2-type bisoxime and terephthalic acid: Synthesis, structure and photophysical properties. *Z. Anorg. Allg. Chem.* **2016**, *642*, 834–839. [CrossRef]
49. Dong, W.K.; Du, W.; Zhang, X.Y.; Li, G.; Dong, X.Y. Synthesis, crystal structure and spectral properties of a supramolecular trinuclear nickel(II) complex with 5-methoxy-4′-bromo-2,2′-[ethylenedioxybis(nitrilomethylidyne)]diphenol. *Spectrochim. Acta Part A* **2014**, *132*, 588–593. [CrossRef] [PubMed]
50. Wang, P.; Zhao, L. An infinite 2D supramolecular cobalt(II) complex based on an asymmetric Salamo-type ligand: Synthesis, crystal structure, and spectral properties. *Synth. React. Inorg. Met.-Org. Nano-Met. Chem.* **2016**, *46*, 1095–1101. [CrossRef]
51. Wang, P.; Zhao, L. Synthesis, structure and spectroscopic properties of the trinuclear cobalt(II) and nickel(II) complexes based on 2-hydroxynaphthaldehyde and bis(aminooxy)alkane. *Spectrochim. Acta Part A* **2015**, *135*, 342–350. [CrossRef] [PubMed]
52. Dong, X.Y.; Kang, Q.P.; Jin, B.X.; Dong, W.K. A dinuclear nickel(II) complex derived from an asymmetric salamo-type N_2O_2 chelate ligand: Synthesis, structure and optical properties. *Z. Naturforsch.* **2017**, *72*, 415–420. [CrossRef]

53. Wu, H.L.; Pan, G.L.; Wang, H.; Wang, X.L.; Bai, Y.C.; Zhang, Y.H. Study on synthesis, crystal structure, antioxidant and DNA-binding of mono-, di- and poly-nuclear lanthanides complexes with bis(*N*-salicylidene)-3-oxapentane-1,5-diamine. *J. Photochem. Photobiol. B* **2014**, *135*, 33–43. [CrossRef] [PubMed]
54. Ma, J.C.; Dong, X.Y.; Dong, W.K.; Zhang, Y.; Zhu, L.C.; Zhang, J.T. An unexpected dinuclear Cu(II) complex with a bis(salamo) chelating ligand: Synthesis, crystal structure and photophysical properties. *J. Coord. Chem.* **2016**, *69*, 149–159. [CrossRef]
55. Wu, H.L.; Bai, Y.C.; Zhang, Y.H.; Li, Z.; Wu, M.C.; Chen, C.Y.; Zhang, J.W. Synthesis, crystal structure, antioxidation and DNA-binding properties of a dinuclear copper(II) complex with bis(*N*-salicylidene)-3-oxapentane-1,5-diamine. *J. Coord. Chem.* **2014**, *67*, 3054–3066. [CrossRef]
56. Hu, J.H.; Sun, Y.; Qi, J.; Li, Q.; Wei, T.B. A new unsymmetrical a zine derivative based on coumarin group as dual-modal sensor for CN^-, and fluorescent "off-on" for Zn^{2+}. *Spectrochim. Acta A* **2017**, *175*, 125–133. [CrossRef] [PubMed]
57. Wu, H.L.; Pan, G.L.; Bai, Y.C.; Wang, H.; Kong, J. Synthesis, structure, antioxidation, and DNA-bindingstudies of a binuclear ytterbium(III) complex with bis(N-salicylidene) -3-oxapentane-1,5-diamine. *Res. Chem. Intermed.* **2015**, *41*, 3375–3388. [CrossRef]
58. Liu, P.P.; Wang, C.Y.; Zhang, M.; Song, X.Q. Pentanuclear sandwich-type Zn^{II}-Ln^{III} clusters based on a new salen-like salicylamide ligand: Structure, near-infrared emission and magnetic properties. *Polyhedron* **2017**, *129*, 133–140. [CrossRef]
59. Song, X.Q.; Peng, Y.J.; Chen, G.Q.; Wang, X.R.; Liu, P.P.; Xu, W.Y. Substituted group-directed assembly of Zn(II) coordination complexes based on two new structural related pyrazolone based Salen ligands: Syntheses, structures and fluorescence properties. *Inorg. Chim. Acta* **2015**, *427*, 13–21. [CrossRef]
60. Wang, F.; Liu, L.Z.; Gao, L.; Dong, W.K. Unusual constructions of two salamo-based copper(II) complexes. *Spectrochim. Acta Part A* **2018**, *203*, 56–64. [CrossRef] [PubMed]
61. Wu, H.L.; Bai, Y.C.; Zhang, Y.H.; Pan, G.L.; Kong, J.; Shi, F.; Wang, X.L. Two lanthanide(III) complexes based on the Schiff base *N*,*N*-Bis(salicylidene)-1,5-diamino-3-oxapentane: Synthesis, characterization, DNA-binding properties, and antioxidation. *Z. Anorg. Allg. Chem.* **2014**, *640*, 2062–2071. [CrossRef]
62. Song, X.Q.; Liu, P.P.; Liu, Y.A.; Zhou, J.J.; Wang, X.L. Two dodecanuclear heterometallic $[Zn_6Ln_6]$ clusters constructed by a multidentate salicylamide salen-like ligand: Synthesis, structure, luminescence and magnetic properties. *Dalton Trans.* **2016**, *45*, 8154–8163. [CrossRef] [PubMed]
63. Hu, J.H.; Chen, J.J.; Li, J.B.; Qi, J. A cyanide ion probe based on azosalicylic aldehyde of benzoyl hydrazone. *Chin. J. Inorg. Chem.* **2014**, *30*, 2544–2548.
64. Gao, L.; Liu, C.; Wang, F.; Dong, W.K. Tetra-, penta- and hexa-coordinated transition metal complexes constructed from coumarin-cntaining N_2O_2 ligand. *Crystals* **2018**, *8*, 77. [CrossRef]
65. Song, X.Q.; Liu, P.P.; Xiao, Z.R.; Li, X.; Liu, Y.A. Four polynuclear complexes based on a versatile salicylamide salen-like ligand: Synthesis, structural variations and magnetic properties. *Inorg. Chim. Acta* **2015**, *438*, 232–244. [CrossRef]
66. Li, X.Y.; Kang, Q.P.; Liu, L.Z.; Ma, J.C.; Dong, W.K. Trinuclear Co(II) and mononuclear Ni(II) Salamo-type bisoxime coordination compounds. *Crystals* **2018**, *8*, 43. [CrossRef]
67. Guo, W.T.; Li, X.Y.; Kang, Q.P.; Ma, J.C.; Dong, W.K. Structural and luminescent properties of heterobimetallic zinc(II)-europium(III) dimer constructed from N_2O_2-type bisoxime and terephthalic acid. *Crystals* **2018**, *8*, 154. [CrossRef]
68. Hao, J.; Li, X.Y.; Zhang, Y.; Dong, W.K. A reversible bis(salamo)-based fluorescence sensor for selective detection of Cd^{2+} in water-containing systems and food samples. *Materials* **2018**, *11*, 523. [CrossRef] [PubMed]
69. Zhang, L.W.; Li, X.Y.; Kang, Q.P.; Ma, J.C.; Dong, W.K. Structures and fluorescent and magnetic behaviors of newly synthesized Ni^{II} and Cu^{II} coordination compounds. *Crystals* **2018**, *8*, 173. [CrossRef]
70. Dong, X.Y.; Kang, Q.P.; Li, X.Y.; Ma, J.C.; Dong, W.K. Structurally characterized solvent-induced homotrinuclear cobalt(II) N_2O_2-donor bisoxime-type complexes. *Crystals* **2018**, *8*, 139. [CrossRef]
71. Yang, Y.H.; Hao, J.; Li, X.Y.; Zhang, Y.; Dong, W.K. Hetero-trinuclear $Co^{II}{}_2$-Dy^{III} complex with a octadentate bis(salamo)-like ligand: Synthesis, crystal structure and luminescence properties. *Crystals* **2018**, *8*, 174. [CrossRef]

72. Kruszynski, R.; Sieranski, T. Can stacking interactions exist beyond the commonly accepted limits? *Cryst. Growth Des.* **2016**, *16*, 587–595. [CrossRef]
73. Bernstein, J.; Davis, R.E.; Shimoni, L.; Chang, N.L. Patterns in hydrogen bonding: Functionality and graph set analysis in crystals. *Angew. Chem. Int. Ed. Engl.* **1995**, *34*, 1555–1573. [CrossRef]
74. McKinnon, J.J.; Jayatilaka, D.; Spackman, M.A. Towards quantitative analysis of intermolecular interactions with Hirshfeld surfaces. *Chem. Commun.* **2007**, 3814–3816. [CrossRef]
75. Spackman, M.A.; McKinnon, J.J.; Jayatilaka, D. Electrostatic potentials mapped on Hirshfeld surfaces provide direct insight into intermolecular interactions in crystals. *Cryst. Eng. Commun.* **2008**, *10*, 377–388. [CrossRef]
76. Spackman, M.A.; Jayatilaka, D. Hirshfeld surface analysis. *Cryst. Eng. Commun.* **2009**, *11*, 19–32. [CrossRef]
77. Martin, A.D.; Hartlieb, K.J.; Sobolev, A.N.; Raston, C.L. Hirshfeld surface analysis of substituted phenols. *Cryst. Growth Des.* **2010**, *10*, 5302–5306. [CrossRef]
78. Chattopadhyay, B.; Mukherjee, A.K.; Narendra, N.; Hemantha, H.P.; Sureshbabu, V.V.; Helliwell, M.; Mukherjee, M. Supramolecular architectures in 5,5′-substituted hydantoins: Crystal structures and Hirshfeld surface analyses. *Cryst. Growth Des.* **2010**, *10*, 4476–4484. [CrossRef]
79. Liu, Y.A.; Wang, C.Y.; Zhang, M.; Song, X.Q. Structures and magnetic properties of cyclic heterometallic tetranuclear clusters. *Polyhedron* **2017**, *127*, 278–286. [CrossRef]
80. Dong, Y.J.; Ma, J.C.; Zhu, L.C.; Dong, W.K.; Zhang, Y. Four 3d–4f heteromultinuclear zinc(II)-lanthanide(III) complexes constructed from a distinct hexadentate N_2O_2-type ligand: Syntheses, structures and photophysical properties. *J. Coord. Chem.* **2017**, *70*, 103–115. [CrossRef]
81. Dong, W.K.; Ma, J.C.; Zhu, L.C.; Zhang, Y.; Li, X.L. Four new nickel(II) complexes based on an asymmetric Salamo-type ligand: Synthesis, structure, solvent effect and electrochemical property. *Inorg. Chim. Acta* **2016**, *445*, 140–148. [CrossRef]
82. Dong, W.K.; Lan, P.F.; Zhou, W.M.; Zhang, Y. Salamo-type trinuclear and tetranuclear cobalt(II) complexes based on a new asymmetry salamo-type ligand: Syntheses, crystal structures and fluorescence properties. *J. Coord. Chem.* **2016**, *65*, 1272–1283. [CrossRef]
83. Dong, W.K.; Zhang, J.T.; Dong, Y.J.; Zhang, Y.; Wang, Z.K. Construction of mononuclear copper(II) and trinuclear cobalt(II) complexes based on asymmetric salamo-type ligands. *Z. Anorg. Allg. Chem.* **2016**, *642*, 189–196. [CrossRef]
84. Wang, L.; Hao, J.; Zhai, L.X.; Zhang, Y.; Dong, W.K. Synthesis, crystal structure, luminescence, electrochemical and antimicrobial properties of bis(salamo)-based Co(II) complex. *Crystals* **2017**, *7*, 277. [CrossRef]